行政院國家科學委員會補助專題研究計畫 □成果報告
■期中進度報告

電漿改質之單層奈米碳管的研究與應用

計畫類別：■ 個別型計畫　□ 整合型計畫
計畫編號：NSC 98 － 2221 － E － 034 － 007 － MY2
執行期間： 98 年 8 月 1 日至 100 年 7 月 31 日

計畫主持人：施漢章
共同主持人：
計畫參與人員：劉峻幗

成果報告類型(依經費核定清單規定繳交)：■精簡報告　□完整報告

本成果報告包括以下應繳交之附件：
□赴國外出差或研習心得報告一份
□赴大陸地區出差或研習心得報告一份
■出席國際學術會議心得報告及發表之論文各一份
□國際合作研究計畫國外研究報告書一份

處理方式：除產學合作研究計畫、提升產業技術及人才培育研究計畫列管計畫及下列情形者外，得立即公開查詢
■涉及專利或其他智慧財產權，□一年■二年後可公開查詢

執行單位：中國文化大學化學工程與材料工程學系奈米材料所

中　華　民　國 99 年 5 月 31 日

中文摘要

氧與氟改質的單層奈米碳管是由微波電漿輔助化學氣相沉積系統所製造，且被用來製作一種新穎的氣體感測器材料。在室溫下對 100 ppm 酒精的感測特性為一電阻提升的 P 型反應。氧電漿改質 30 秒能夠讓感測反應由 1.13 提升至 1.74，由掃描式電子顯微鏡與拉曼光譜儀的結果可證明此乃因非晶質碳被明顯的去除。然而氧電漿改質對於降低反應與復原時間並無明顯的功效。利用氟電漿改質 60 秒只能夠讓感測反應由 1.13 提升至 1.51，但反應與復原時間能分別從 178 與 364 秒降至 54 與 97 秒，由 X 光光電子能譜儀與歐傑電子能譜儀的結果可證明此乃因大量含氟官能基存在的關係。因此電將改質的單層奈米碳管能夠提升室溫酒精感測的靈敏度與反應性。

關鍵詞：單層奈米碳管，微波電漿輔助化學氣相沉積系統，表面改質，酒精，氣體感測

Diamond & Related Materials 19 (2010) 981–987

Contents lists available at ScienceDirect

Diamond & Related Materials

journal homepage: www.elsevier.com/locate/diamond

Effect of plasma modification of single wall carbon nanotubes on ethanol vapor sensing

Chun-Kuo Liu [a], Meng-Wen Huang [b], Jyh-Ming Wu [c], Han C. Shih [a,d,*]

[a] Department of Materials Science and Engineering, National Tsing Hua University, Hsinchu 30013, Taiwan
[b] Department of Materials Science and Engineering, National Chung Hsing University, Taichung 40227, Taiwan
[c] Department of Materials Science and Engineering, Feng Chia University, Taichung 40724, Taiwan
[d] Institute of Materials Science and Nanotechnology, Chinese Culture University, Taipei 11114, Taiwan

ARTICLE INFO

Available online 6 March 2010

Keywords:
Single wall carbon nanotubes (SWCNTs)
Microwave plasma enhanced chemical vapor deposition (MPECVD)
Surface modification
Resistance
Ethanol
Gas sensor

ABSTRACT

The oxygen and fluorine modified single wall carbon nanotubes (SWCNTs) were manufactured by microwave plasma enhanced chemical vapor deposition (MPECVD), and were developed as novel gas sensor materials. The sensor characteristic has shown a p-type response with resistance enhancement upon exposure to 100 ppm ethanol at room temperature. Oxygen plasma modification can increase the sensor response from 1.13 to 1.74 on process duration of 30 s due to the apparent elimination of amorphous carbon, as demonstrated by FESEM and Raman results. However, oxygen plasma modification has no effective assistance in decreasing the response and recovery time. By applying fluorine plasma modification, the sensor response only increases from 1.13 to 1.51 on process duration of 60 s, but the response and recovery time can decrease apparently from 178 to 54 s and 364 to 97 s due to the existence of numerous fluorine-included functional groups, as demonstrated by XPS and AES results. Therefore, the plasma modified SWCNT can elevate the sensitivity and reactivity for room temperature ethanol sensing.

1. Introduction

The discovery of carbon nanotubes (CNTs) was in 1991 [1], and single wall carbon nanotubes (SWCNTs) were discovered two years later [2]. Outstanding physical, chemical, mechanical and electrical properties have been gradually researched due to their unique structure [3–5]. Many important applications have been demonstrated, and both CNT-based [6–14] and CNT-doped [15–20] gas sensors received considerable attention because of their nanometer hollow geometry, high specific surface area, high electron mobility, surface modifications and functionalizations.

Ethanol sensors have wide applications in traffic safety, foodstuffs, fermentation processes, and alcoholic beverage production processes. Several different sensing technologies, including optic [21], surface acoustic wave [22], and resistiveness [6–20], have been used to detect ethanol concentrations. Among the various types of sensors, the resistive method has the advantages of simplicity of construction, low cost, and popular applications.

Semiconductor metal oxide (e.g., SnO_2) is often used as an ethanol sensor, but generally it requires a high working temperature exceeding 300 °C [15]. CNT-based ethanol sensors may work at room temperature and have a quite low detection limit; however, they exhibit a lower sensitivity due to fewer percentages of semiconducting nanotubes that can be modulated by gas molecules. Besides, the recovery time of CNT-based ethanol sensors is actually long because of the strong adsorption between CNTs and gas molecules [8–10]. In this work, how to enhance the selectivity and reactivity of SWCNT-based ethanol sensors is our major purpose.

2. Experimental

2.1. Materials

The CarboLex AP-grade SWCNTs used in this work were commercially obtained by Sigma-Aldrich Co. (No. 519308). The product was made by arc method in specifically designed chambers. These SWCNTs are of average diameter ~1.5 nm and are found in bundles which are typically ~20 nm in diameter with lengths of 2–5 μm. The purity of the AP-grade SWCNTs is 50–70 vol.%, and the impurities include ~35 wt.% residual catalysts (Ni, Y) and some amorphous carbons. The SWCNTs include both semiconducting (~2/3) and metallic (~1/3) nanotubes demonstrated by electron diffraction measurements of TEM and atomic resolution STM. The SWCNTs dispersed in an ethanol solution were dropped onto a non-conductive alumina substrate quantitatively. Microwave plasma enhanced chemical vapor deposition (MPECVD) was used for surface plasma modification of the SWCNTs. The mixture gases of 20 sccm oxygen

* Corresponding author. Department of Materials Science and Engineering, National Tsing Hua University, Hsinchu 30013, Taiwan. Tel.: +886 3 5715131x33845; fax: +886 3 5710290.
E-mail address: hcshih@mx.nthu.edu.tw (H.C. Shih).

0925-9635/$ – see front matter © 2010 Elsevier B.V. All rights reserved.
doi:10.1016/j.diamond.2010.03.003

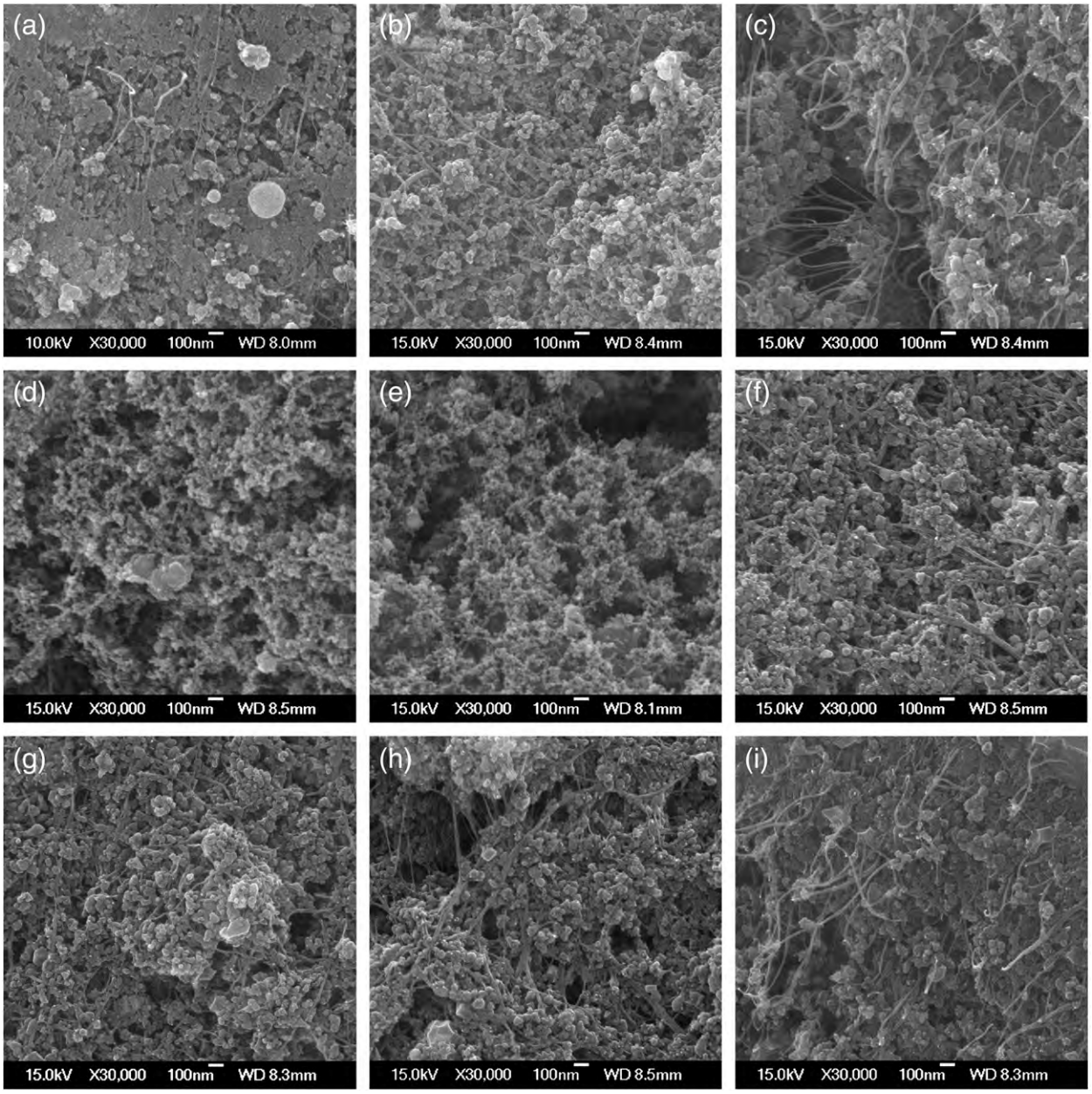

Fig. 1. FESEM images of SWCNT films; (a) untreated, (b–e) treated by oxygen plasma for 15, 30, 45, and 60 s, and (f–i) treated by fluorine plasma for 15, 30, 45, and 60 s.

and 100 sccm argon were introduced for the oxygen plasma treatment, and the mixture gases of 20 sccm tetrafluoromethane (CF_4) and 100 sccm argon were introduced for the fluorine plasma treatment. The operation conditions were described as follows: microwave power of 500 W, operating pressure of 10 Torr, process duration of 15–60 s, and average sample temperature of ~30 °C.

2.2. Characterizations

The morphologies of the plasma modified SWCNT film were characterized by field emission scanning electron microscope (FESEM, JEOL JSM-6500F). The Raman spectra of the plasma modified SWCNTs were characterized by Raman spectrometer (HORIBA Jobin Yvon LabRAM HR800 UV) with a 632.8 nm (1.96 eV) He–Ne laser. The elemental composition change and relevant chemical bonding of the SWCNT film during the plasma treatments were investigated by X-ray photoelectron spectroscopy (XPS, ULVAC-PHI PHI Quantera SXM) with a hemispherical capacitor analyzer. A monochromatic Al Ka line ($h\upsilon = 1486.6$ eV) was used as the photon source, and photoelectrons were collected at an angle of 45° relative to the sample surface. The energy resolution of system (source + analyzer) was 0.49 eV and the elemental detection limit was 0.1 at.%. In the spectrum analysis, the background signal was subtracted by Shirley's method. In order to determine the elemental composition change of a SWCNT bundle during the plasma treatments, Auger electron spectroscopy (AES, ULVAC-PHI PHI-700) with a coaxial cylindrical mirror analyzer was applied to exacter analysis. The Schottky field emission electron source provided a high voltage electron beam (0.1 ~ 25 kV) with a diameter of less than 6 nm for secondary electron imaging. The energy resolution of system was 0.5 eV and the elemental detection limit was down to 0.01 at.%. Before XPS and AES measurements, all samples were presputtered by argon ion beam in order to remove surface contamination (C and O) and acquire true elemental composition.

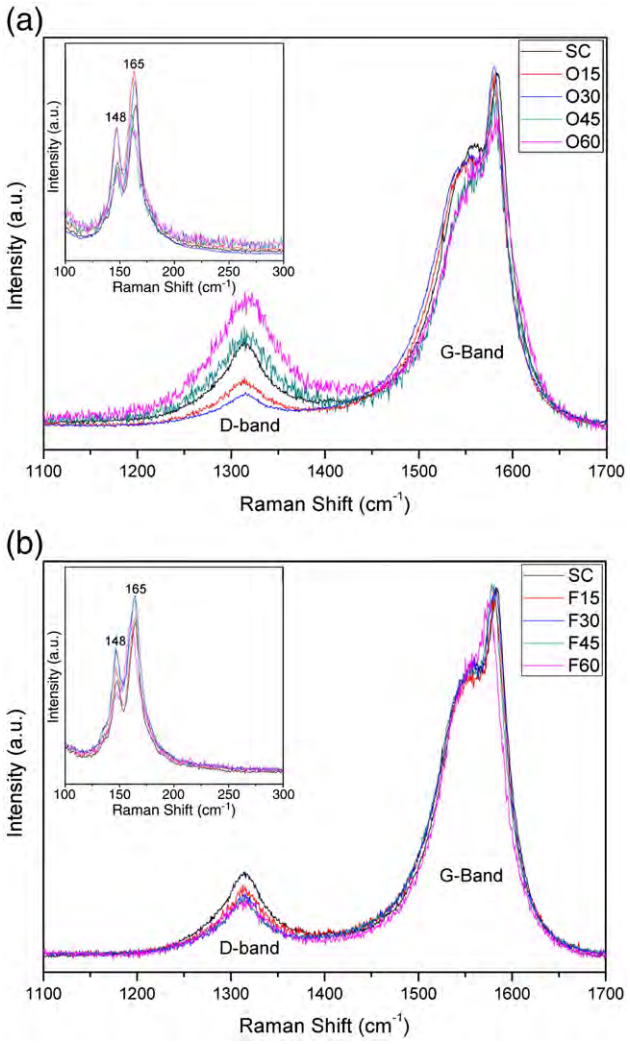

Fig. 2. Raman spectra of SWCNTs (a) treated by oxygen plasma for 0, 15, 30, 45, and 60 s, and (b) treated by fluorine plasma for 0, 15, 30, 45, and 60 s. The inset shows the low-frequency range (radial breathing mode, RBM) of Raman spectra.

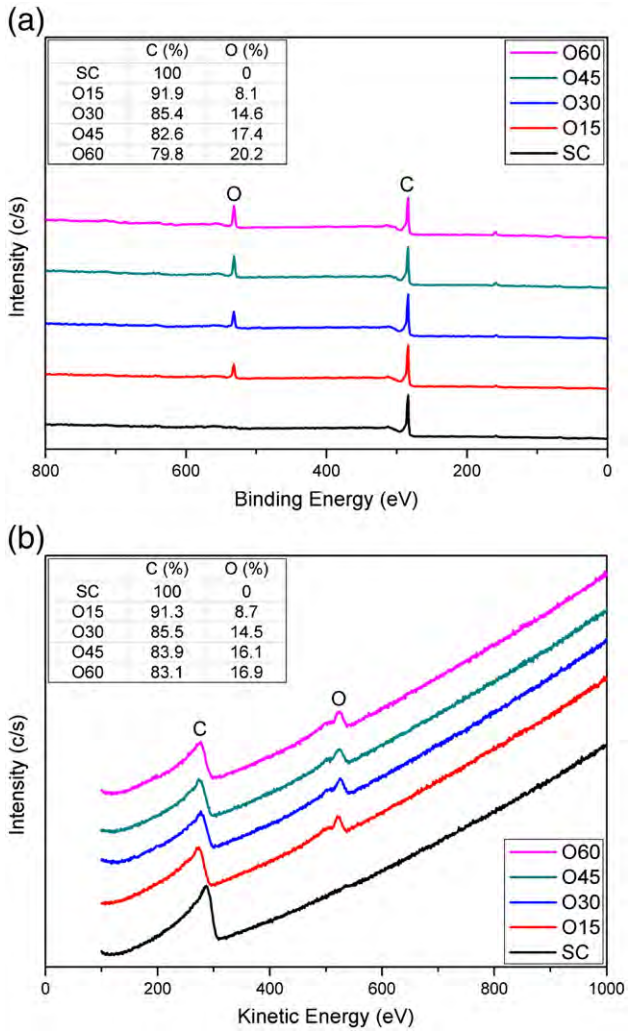

Fig. 3. Survey spectra of SWCNTs treated by oxygen plasma for 0, 15, 30, 45, and 60 s; (a) XPS survey spectra, and (b) AES survey spectra. The inset shows elemental composition change of oxygen plasma treated SWCNTs.

2.3. Gas-sensing measurements

During the gas-sensing test, the resistance (or current) response with a fixed bias of 2 V was monitored by a precision electrochemical workstation (JIEHAN ECW-5000) which can be used to detect a very low current ($\sim 10^{-12}$ A). The test ethanol concentration (100–500 ppm) was obtained by volatile ethanol and subsequently injected into the chamber. After reaching a steady current response, the chamber was purged with air and the experiment was repeated for the next cycle. All sensing experiments were done at 25 ± 0.5 °C, and humidity was kept at $60 \pm 5\%$ RH. The sensor response (S) was defined as $S = R_{gas}/R_{air}$, where R_{gas} and R_{air} were the resistances in an environment containing ethanol vapor and in air ambient, respectively.

3. Results and discussion

3.1. FESEM images

Fig. 1 shows the surface morphology of the SWCNT films with various plasma modifications. In Fig. 1(a), the impurities including 13.12 wt.% amorphous carbons by thermogravimetric analysis (TGA) and residual catalysts (15.62 wt.% Ni, 4.23 wt.% Y) confirmed by energy dispersive spectrometer (EDS) attached on FESEM exist in the commercial SWCNTs. When the SWCNT films were treated by oxygen plasma for 15 and 30 s, the fragile amorphous carbons on the surface are apparently removed and the SWCNTs are observed more clearly, as illustrated in Fig. 1(b) and (c). When the SWCNT films were treated by oxygen plasma for 45 and 60 s, the SWCNTs are destroyed and the appearance of SWCNTs aren't easily distinguished, as illustrated in Fig. 1(d) and (e). Briefly, the SWCNTs can be purified by appropriate oxygen plasma treatment, and the better operation condition in this work is process duration of 30 s.

In Fig. 1(f)–(i), the SWCNTs are still observed clearly when the SWCNT films were treated by fluorine plasma until 60 s. The more distinct SWCNTs after being treated by fluorine plasma show that fluorine plasma treatment can eliminate amorphous carbon more lightly without serious destruction, and the better operation condition in this work is process duration of 60 s.

3.2. Raman spectra

Raman spectroscopy has provided an exceedingly powerful tool in probing the structure (diameter and chirality) and electronic properties

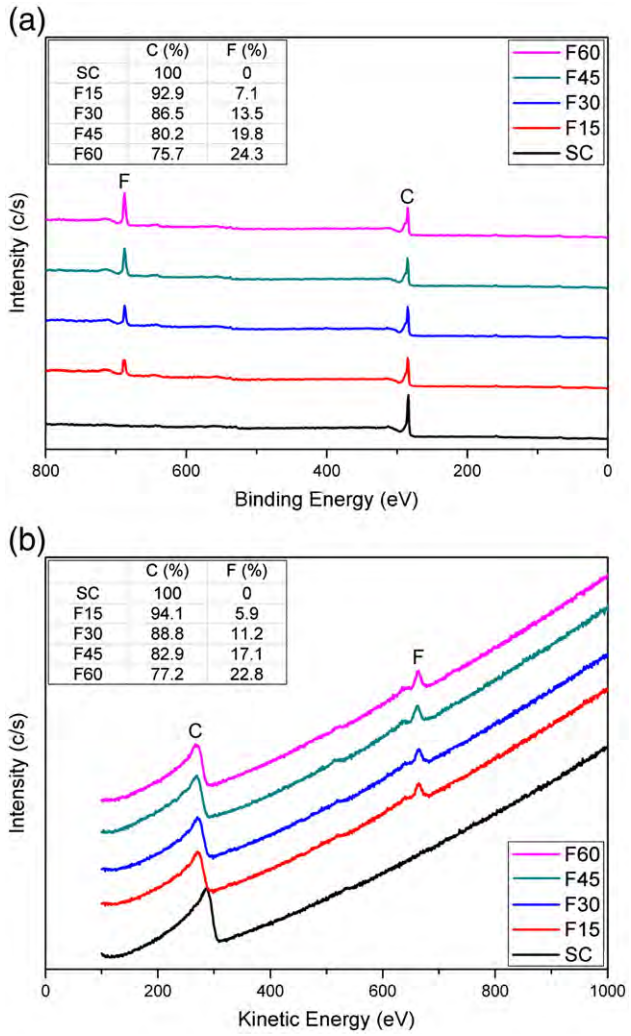

Fig. 4. Survey spectra of SWCNTs treated by fluorine plasma for 0, 15, 30, 45, and 60 s; (a) XPS survey spectra, and (b) AES survey spectra. The inset shows elemental composition change of fluorine plasma treated SWCNTs.

(metallic or semiconducting) of SWCNTs. In contrast to the G-band of highly oriented pyrolytic graphite (HOPG) which exhibits a single peak at 1582 cm^{-1} related to the E_{2g} tangential mode, the G-band of SWCNTs splits into two peaks, G^+ (>1582 cm^{-1}) and G^- (<1582 cm^{-1}), as illustrated in Fig. 2. Fig. 2 also indicates that the D-band of SWCNTs exhibits a single peak at ~1320 cm^{-1} related to the disorder-induced feature. The D-band doesn't occur in HOPG; hence the ratio of the D-band intensity (I_D) to G-band intensity (I_G) represents the disorder level of SWCNTs. The smaller I_D/I_G ratio means that the SWCNTs possess fewer defects in the carbon structure or reduced amorphous carbons remain on the surface of the SWCNT films. From the results of Fig. 2(a), the I_D/I_G ratio of SWCNTs treated by oxygen plasma for 0 (SC), 15 (O15), 30 (O30), 45 (O45), and 60 s (O60) are 0.26, 0.16, 0.11, 0.31, and 0.42, respectively. O15 and O30 have smaller I_D/I_G ratio than SC, but O45 and O60 are in the opposite trend due to the destruction of SWCNTs. From the results of Fig. 2(b), the I_D/I_G ratio of SWCNTs treated by fluorine plasma for 0 (SC), 15 (F15), 30 (F30), 45 (F45), and 60 s (F60) are 0.26, 0.21, 0.18, 0.16, and 0.15, respectively. Therefore, O30 and F60 have the smallest I_D/I_G ratio (or fewest residual amorphous carbons), which conforms to the FESEM results.

The A_{1g} mode in low-frequency range (100–300 cm^{-1}) called radial breathing mode (RBM) is unique to SWCNTs, as illustrated in the inset of Fig. 2. The RBM frequency can be used to study the tube diameter by the relation $\omega = 234/d + 10$ for SWCNT bundles, where ω is the RBM frequency in cm^{-1} and d is the tube diameter in nm [23]. According to the above formula, the diameters of commercial SWCNTs are calculated in the range of 1.5–1.7 nm. In addition, plasma treatments don't seem to concern with tube diameter, but only affect the percentage of SWCNTs with different diameters.

3.3. Survey spectra of XPS and AES

In Fig. 3(a), the XPS survey spectra of oxygen plasma treated SWCNT films reveal the presence of carbon and oxygen, and the oxygen atomic percentage can reach to 14.6% and 20.2% when oxygen plasma treated for 30 and 60 s. The same trend is also observed in AES survey spectra of a SWCNT bundle, as illustrated in Fig. 3(b). The oxygen atomic percentage of O15 and O30 by AES is similar to the results by XPS, but the oxygen atomic percentage of O45 and O60 by AES is slightly lower than the results by XPS, as tabled in the inset of Fig. 3. The variation may result from the destruction of SWCNTs by excess oxygen plasma treatment.

In Fig. 4(a), the XPS survey spectra of fluorine plasma treated SWCNT films reveal the presence of carbon and fluorine, and the atomic concentration of fluorine can reach up to 24.3% when fluorine plasma treated for 60 s. The same trend is also observed in AES survey spectra of a SWCNT bundle, as illustrated in Fig. 4(b). However, the fluorine atomic percentage by AES is slightly lower than the results by XPS, as tabled in the inset of Fig. 4. The probable reason is that fluorine plasma may not easily functionalize on SWCNTs as amorphous carbons.

3.4. Analysis of XPS C_{1s} spectra

Fig. 5(a) shows the XPS C_{1s} spectra of SC, O60, and F60; the XPS C_{1s} peak fitting of the three different kinds of SWCNTs are illustrated in Fig. 5(b)–(d) respectively. In Fig. 5(c), the C_{1s} core level can be decomposed into five components [24]. The peak at 283.9 eV (1) corresponds to the graphite-like sp^2 carbon which indicates the graphite level. The peak at 284.8 eV (2) is attributed to the diamond-like sp^3 carbon which indicates the disorder level. The peaks at 286.0 (3), 288.1 (4), and 289.8 eV (5) correspond to hydroxyl (or ether), carbonyl, and carboxyl (or ester) groups, respectively. After quantitative analysis, relative percentages of the components of carbon atoms are listed in Table 1. O15 and O30 have lower sp^3 carbon percentage than SC, but O45 and O60 show the opposite trend. In addition, the oxygen-bonded carbon percentage can increase to a saturation value (~27%) after 30 s oxygen plasma treatment. Therefore, O30 has least disorder (10.4%) conformed to the Raman results and maximum oxygen-included functional groups. It's noted that the C_{1s} core level of commercial SWCNTs can only be decomposed into two contributions, as illustrated in Fig. 5(b).

In Fig. 5(d), the C_{1s} core level can be decomposed into six components [25]. The peaks at 284.5 (1) and 285.7 eV (2) correspond to the sp^2 and sp^3 carbon, respectively, but the binding energy slightly shifts toward higher energy by comparing to the commercial SWCNTs due to the fluorination of carbon atoms. The peaks related to CF_x groups at 287.0 (3), 288.9 (4), 291.0 (5), and 293.1 eV (6) are ascribed to C–CF_n ($0<n<1$), CF, CF_2, and CF_3 groups, respectively. After quantitative analysis, relative percentages of the components of carbon atoms are listed in Table 2. F60 has least disorder (12.7%) which is consistent with the Raman results and maximum fluorine-included functional groups (40.0%).

3.5. Ethanol-sensing properties

It has been reported that SWCNTs act like a p-type semiconductor when used as sensing materials [8–10]. If an oxidizing gas (e.g. O_2, O_3, and

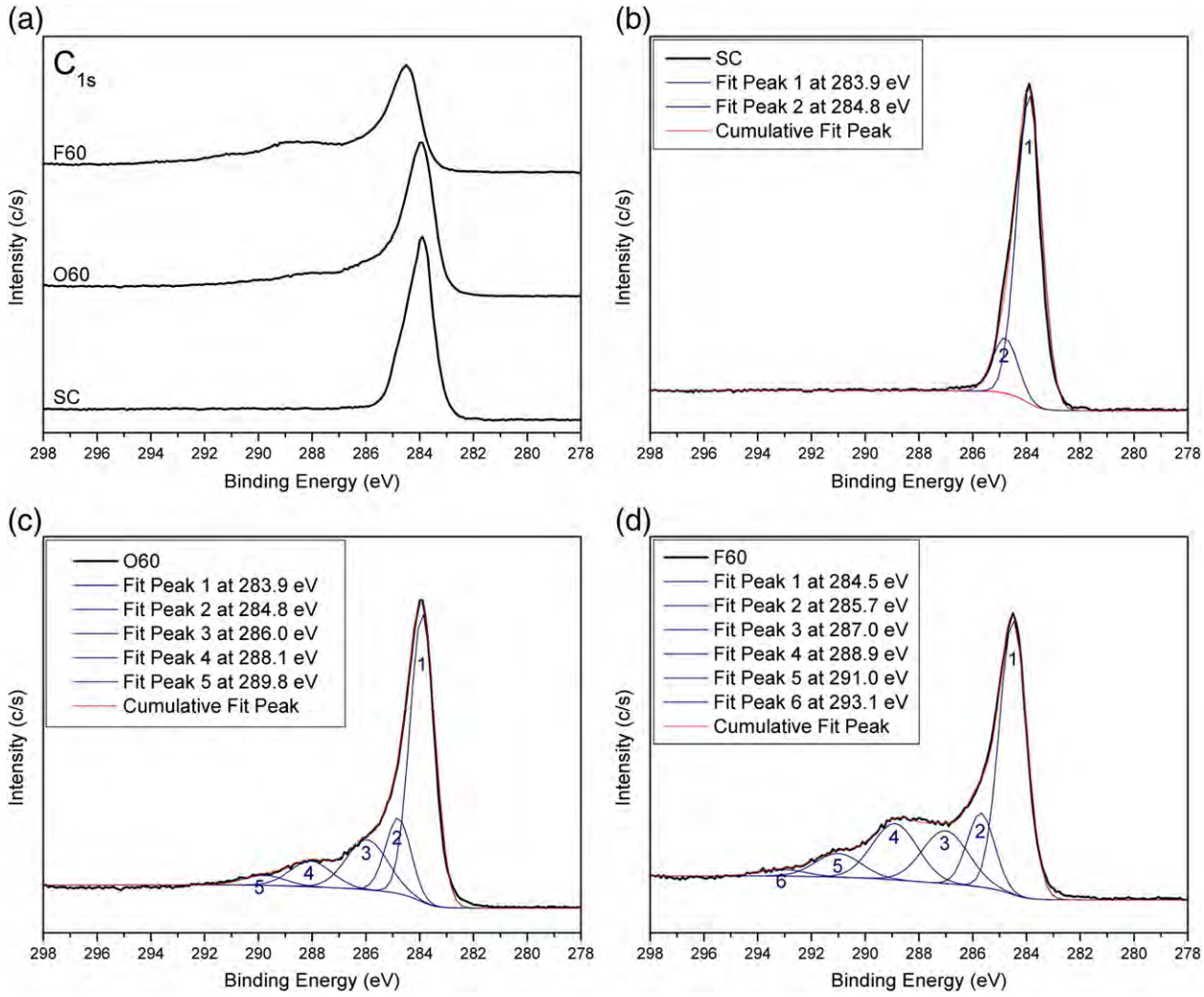

Fig. 5. (a) Comparison between the XPS C_{1s} spectra of three different kinds of SWCNTs. The XPS C_{1s} peak fitting of three different kinds of SWCNTs; (b) untreated, (c) treated by oxygen plasma for 60 s, and (d) treated by fluorine plasma for 60 s. Black lines expresses the raw experimental data. Blue lines are the recommended fitting curves, and the binding energy of recommended fitting peaks is listed in the inset respectively. Red line is the cumulative fitting curve similar to raw experimental curve.

NO_2) chemisorbs on p-type SWCNTs, the electron transfers from material to gas (electrons acceptor) and increases the hole concentration in SWCNTs to cause resistance reduction. While a reducing gas (e.g. H_2, NH_3, and C_2H_5OH) physisorbs on p-type SWCNTs, the electron transfers from gas (electrons donor) to material and decreases the hole concentration in SWCNTs to cause resistance enhancement, as illustrated in Fig. 6. It's noted that the baseline raises up slightly in the repeat test since some irreversible adsorption may occur on the SWCNT surface. From the results of Fig. 6, the sensor response (R_{gas}/R_{air}), response and recovery time to 100 ppm ethanol can be identified, and the data of all kinds of SWCNTs in this work are listed in Table 3.

The sensor response increases apparently by both oxygen and fluorine plasma treatments. The enhancement by oxygen plasma treatment is larger than that by fluorine plasma treatment due to the more powerful ability of amorphous carbon elimination, but the sensor response will decrease after 30 s of oxygen plasma treatment

Table 1
Elemental composition change of SWCNTs treated by oxygen plasma for 0, 15, 30, 45, and 60 s, and relative percentage of the five XPS components of carbon atoms computed from Fig. 5(c).

	C (%)	O (%)	Fit peak 1	Fit peak 2	Fit peak 3	Fit peak 4	Fit peak 5
			sp^2 carbon (%) graphite-like	sp^3 carbon (%) diamond-like	C–O (%) hydroxyl groups	C=O (%) carbonyl groups	COO (%) carboxyl groups
SC	100	0	84.8	15.2	0	0	0
O15	91.9	8.1	73.3	12.7	8.1	3.8	2.1
O30	85.4	14.6	62.8	10.4	14.2	7.4	5.2
O45	82.6	17.4	60.1	13.2	15.5	7.6	3.6
O60	79.8	20.2	57.2	15.0	16.2	8.3	3.3

Table 2
Elemental composition change of SWCNTs treated by fluorine plasma for 0, 15, 30, 45, and 60 s, and relative percentage of the six XPS components of carbon atoms computed from Fig. 5(d).

	C (%)	F (%)	Fit peak 1	Fit peak 2	Fit peak 3	Fit peak 4	Fit peak 5	Fit peak 6
			sp^2 carbon (%) graphite-like	sp^3 carbon (%) diamond-like	$C–CF_n$ (%) $0<n<1$	CF (%)	CF_2 (%)	CF_3 (%)
SC	100	0	84.8	15.2	0	0	0	0
F15	92.9	7.1	70.8	14.7	6.1	5.8	2.1	0.5
F30	86.5	13.5	59.0	13.4	12.2	11.4	3.2	0.8
F45	80.2	19.8	50.7	13.2	14.5	14.6	5.6	1.4
F60	75.7	24.3	47.3	12.7	15.2	16.1	6.8	1.9

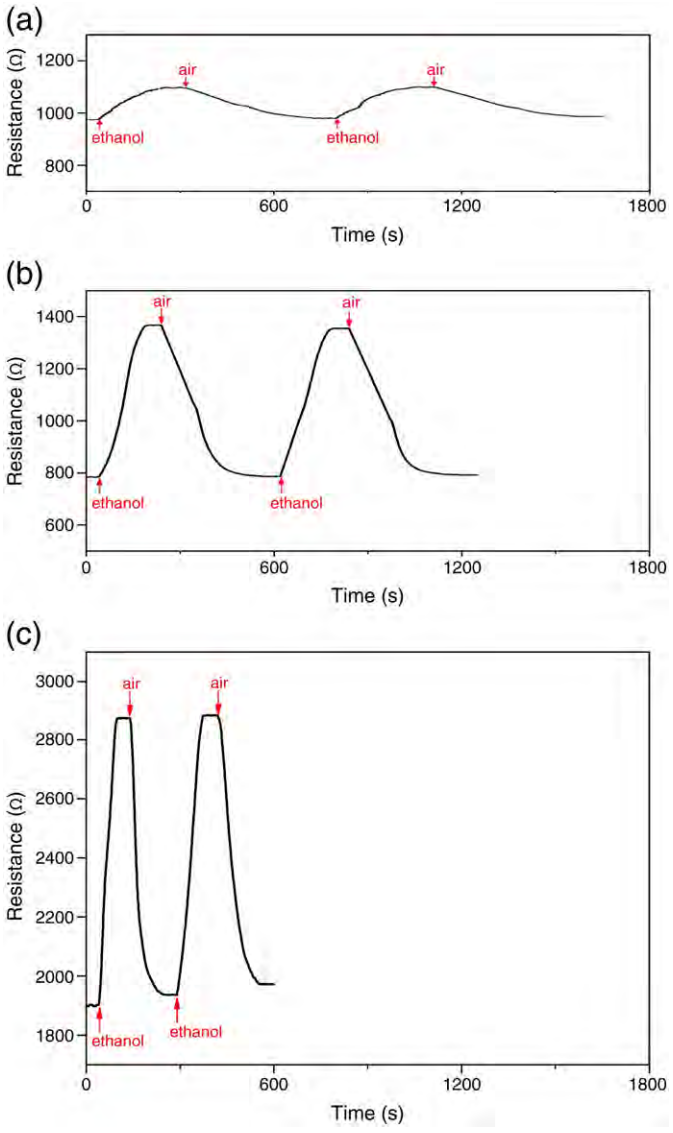

Fig. 6. The resistance response to 100 ppm ethanol of three different kinds of SWCNTs at operating conditions of 25 ± 0.5 °C and 60 ± 5% RH; (a) untreated, (b) treated by oxygen plasma for 30 s, and (c) treated by fluorine plasma for 60 s. The symbol "ethanol" means ethanol injection, and the symbol "air" means air purge.

as a result of SWCNTs destruction, which is consistent with the FESEM results. Therefore, O30 and F60 have the maximum sensor response of 1.74 and 1.51 than SC (1.13).

In theory, ethanol molecules physisorb on SWCNTs by van der Waals force; hence the response and recovery time are very slow. The response and recovery time decrease evidently by both oxygen and fluorine plasma treatments, and the reduction by fluorine plasma treatment is larger than that by oxygen plasma treatment. The faster response and recovery may result from the formation of hydrogen bonds ($C_2H_5–O–H\cdots O–C$ and $C_2H_5–O–H\cdots F–C$) instead of van der Waals force. The more attractive bonding of H···F due to the more electronegative F atom accelerates the response time more than H···O. The lower bonding energy of H···F which causes the easier desorption than H···O also accelerates the recovery time [26]. Therefore, F60 can effectively reduce the response and recovery time from 178 to 54 s and 364 to 97 s due to the most fluorine-included functional groups.

Varying the ethanol concentration from 100 to 500 ppm, we rendered the sensor response versus concentration curves in Fig. 7. SC is not relatively sensitive to the concentration variation due to the saturation adsorption of ethanol. O30 and F60 possess the higher sensitivity (sensor response variation/ethanol concentration variation) between 100 and 300 ppm ethanol concentration sensing tests, and they tend to saturation adsorption in higher ethanol concentration. Therefore, plasma modified SWCNTs have better sensitivity and reactivity in suitable detection range for room temperature ethanol sensing, and they don't need quite high working temperature like the conventional gas sensors.

4. Conclusion

The SWCNT-based gas sensors treated by oxygen and fluorine plasma have shown a p-type response with resistance enhancement upon exposure to 100 ppm ethanol at room temperature. Oxygen plasma modification can increase the sensor response from 1.13 to 1.74 on process duration of 30 s due to the apparent elimination of amorphous carbon. However, oxygen plasma modification has no effective assistance in decreasing the response and recovery time. By applying fluorine plasma modification, the sensor response only increases from 1.13 to 1.51 on process duration of 60 s, but the response and recovery time can decrease apparently from 178 to 54 s and 364 to 97 s due to the existence of numerous fluorine-included functional groups. Therefore, the plasma modified SWCNTs have wide potential to apply on room

Table 3
Sensor response, response and recovery time to 100 ppm ethanol of all kinds of SWCNTs in this work. Response time is defined as the time to reach 90% of the equilibrium signal, and recovery time is defined as the time to go back to 90% of the background signal.

	SC	O15	O30	O45	O60	F15	F30	F45	F60
Sensor response (R_{gas}/R_{air})	1.13	1.49	1.74	1.52	1.36	1.25	1.36	1.44	1.51
Response time (s)	178	151	140	158	169	128	113	83	54
Recovery time (s)	364	318	296	329	346	279	208	131	97

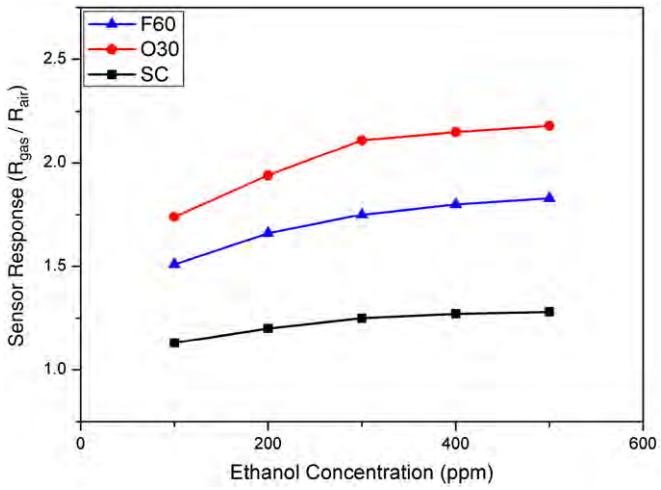

Fig. 7. Comparison between the sensor responses of three different kinds of SWCNTs in varied ethanol concentration sensing tests (100–500 ppm).

temperature gas sensor devices. In the further study, the combination or integration of the oxygen and fluorine plasma modification of SWCNTs may provide a better sensitivity and reactivity for ethanol sensing.

Acknowledgement

The authors would like to thank the National Science Council of the Republic of China (ROC) for the financial support of this work under the contract NSC 96-2221-E-034-006-MY2.

References

[1] S. Iijima, Nature 354 (1991) 56.
[2] S. Iijima, T. Ichihashi, Nature 363 (1993) 603.
[3] M.M.J. Treacy, T.W. Ebbesen, J.M. Gibson, Nature 381 (1996) 678.
[4] P. Delaney, H.J. Choi, J. Ihm, S.G. Louie, M.L. Cohen, Nature 391 (1998) 466.
[5] C.K. Liu, C.T. Hu, Y.H. Yang, Y.S. Chang, H.C. Shih, Diamond Relat. Mater. 18 (2009) 345.
[6] J.K. Nathan, R. Franklin, C. Zhou, M.G. Chapline, S. Peng, K. Cho, H. Dai, Science 287 (2000) 622.
[7] P.G. Collins, K. Bradley, M. Ishigami, A. Zettl, Science 287 (2000) 1801.
[8] P. Qi, O. Vermesh, M. Grecu, A. Javey, Q. Wang, H. Dai, S. Peng, K.J. Cho, Nano Lett. 3 (2003) 347.
[9] T. Someya, J. Small, P. Kim, C. Nuckolls, J.T. Yardley, Nano Lett. 3 (2003) 877.
[10] J. Li, Y. Lu, Q. Ye, M. Cinke, J. Han, M. Meyyappan, Nano Lett. 3 (2003) 929.
[11] L. Valentini, C. Cantalini, I. Armentano, J.M. Kenny, L. Lozzi, S. Santucci, Diamond Relat. Mater. 13 (2004) 1301.
[12] Y. Hayakawa, Y. Suda, T. Hashizume, H. Sugawara, Y. Sakai, Jpn. J. Appl. Phys. 46 (2007) L362.
[13] H.J. Song, Y. Lee, T. Jiang, A.G. Kussow, M. Lee, S. Hong, Y.K. Kwon, H.C. Choi, J. Phys. Chem. C 112 (2008) 629.
[14] C.T. Hu, C.K. Liu, M.W. Huang, S.H. Syue, J.M. Wu, Y.S. Chang, J.W. Yeh, H.C. Shih, Diamond Relat. Mater. 18 (2009) 472.
[15] B.Y. Wei, M.C. Hsu, P.G. Su, H.M. Lin, R.J. Wu, H.J. Lai, Sens. Actuators B 101 (2004) 81.
[16] C. Wei, L. Dai, A. Roy, T.B. Tolle, J. Am. Chem. Soc. 128 (2006) 1412.
[17] L. Niu, Y. Luo, Z. Li, Sens. Actuators B 126 (2007) 361.
[18] N.V. Hieu, N.V. Duy, P.T. Huy, N.D. Chien, Physica E 40 (2008) 2950.
[19] N.V. Duy, N.V. Hieu, P.T. Huy, N.D. Chien, M. Thamilselvan, J. Yi, Physica E 41 (2008) 258.
[20] J. Gong, J. Sun, Q. Chen, Sens. Actuators B 130 (2008) 829.
[21] K. Mitsubayashi, T. Kon, Y. Hashimota, Biosens. Bioelectron. 19 (2003) 193.
[22] M. Penza1, M.A. Tagliente, P. Aversa, M. Re, G. Cassano, Nanotechnol. 18 (2007) 185502.
[23] M.S. Dresselhausa, G. Dresselhaus, R. Saito, A. Jorio, Phys. Rep. 409 (2005) 47.
[24] C. Pirlot, I. Willems, A. Fonseca, J.B. Nagy, Adv. Eng. Mater. 4 (2002) 109.
[25] K.H. An, J.G. Heo, K.G. Jeon, D.J. Bae, C. Jo, C.W. Yang, C.Y. Park, Y.H. Lee, Y.S. Lee, Y.S. Chung, Appl. Phys. Lett. 80 (2002) 4235.
[26] G.R. Desiraju, T. Steiner, The weak hydrogen bond, Structure Chemistry and Biology, Oxford University Press, New York, 2001, p. 16.

可供推廣之研發成果資料表

■ 可申請專利　□ 可技術移轉　日期：99 年 5 月 31 日

國科會補助計畫	計畫名稱：電漿改質之單層奈米碳管的研究與應用 計畫主持人：施漢章 計畫編號：NSC 98-2221-E-034-007-MY2 學門領域：E0699
技術/創作名稱	利用電漿改質的奈米碳管氣體感測器
發明人/創作人	劉峻幗、施漢章
技術說明	中文：
	英文：
可利用之產業及可開發之產品	
技術特點	
推廣及運用的價值	

※ 1. 每項研發成果請填寫一式二份，一份隨成果報告送繳本會，一份送 貴單位研發成果推廣單位（如技術移轉中心）。

※ 2. 本項研發成果若尚未申請專利，請勿揭露可申請專利之主要內容。

※ 3. 本表若不敷使用，請自行影印使用。